



Published in final edited form as:

Cancer Res. 2016 May 1; 76(9): 2513–2524. doi:10.1158/0008-5472.CAN-15-1325.

Elucidation of the roles of tumor integrin $\beta 1$ in the extravasation stage of the metastasis cascade

Michelle B. Chen¹, John M. Lamar², Ran Li³, Richard O. Hynes², and Roger D. Kamm^{1,3}

¹Department of Mechanical Engineering, Massachusetts Institute of Technology, Cambridge, MA, 02139

²Department of Biology, Massachusetts Institute of Technology, Cambridge, MA, 02139

³Department of Biological Engineering, Massachusetts Institute of Technology, Cambridge, MA, 02139

Abstract

Tumor integrin $\beta 1$ (ITGB1) contributes to primary tumor growth and metastasis, but its specific roles have yet been clearly elucidated. In this study, we engineered a three-dimensional microfluidic model of the human microvasculature to recapitulate the environment wherein extravasation takes place and assess the consequences of $\beta 1$ depletion in cancer cells. Combined with confocal imaging, these tools allowed us to decipher the detailed morphology of transmigrating tumor cells and associated endothelial cells in vitro at high spatio-temporal resolution not easily achieved in conventional transmigration assays. Dynamic imaging revealed that $\beta 1$ -depleted cells lacked the ability to sustain protrusions into the subendothelial matrix in contrast to control cells. Specifically, adhesion via $\alpha 3\beta 1$ and $\alpha 6\beta 1$ to subendothelial laminin was a critical prerequisite for successful transmigration. $\beta 1$ was required to invade past the endothelial basement membrane, whereas its attenuation in a syngeneic tumor model resulted in reduced metastatic colonization of the lung, an effect not observed upon depletion of other integrin alpha and beta subunits. Collectively, our findings in this novel model of the vascularized tumor microenvironment revealed a critical requirement for $\beta 1$ in several steps of extravasation, providing new insights into the mechanisms underlying metastasis.

Introduction

Although major advances have been made in the screening and treatment of primary tumors, metastasis still remains the leading cause of cancer-related deaths. For a tumor cell to metastasize successfully, it must first dissociate from the primary tumor, traverse through tumor basement membrane (BM) and stroma, intravasate, survive in the circulation amongst a host of immune cells and mechanical stresses, and lastly, extravasate from the

Correspondence to: Richard O. Hynes; Roger D. Kamm.

Author's contributions

Conception and design: MBC, JML, ROH, RDK Acquisition of data: MBC, JML, RL

Writing, review and revision of manuscript: MBC, JML, ROH, RDK

The authors disclose no potential conflicts of interest.

microvasculature and form metastases in the secondary parenchyma. In particular, the latter steps involving transendothelial migration (TEM) and survival have been described as rate-regulating events in metastasis ^{1,2}.

This complex series of cell-cell and cell-matrix interactions is thought to involve integrins, the family of heterodimeric transmembrane receptors that mediate cellular interactions with the extracellular matrix (ECM). Integrins are widely known to regulate a variety of tumor cell functions including adhesion, migration, invasion, proliferation and survival ³. In particular, the $\beta 1$ subunit forms heterodimers with at least 18 different alpha subunits, and has been shown to bind via its extracellular domain to a substantial number of ECM proteins, and via its intracellular domain to recruit many signaling and cytoskeletal proteins ⁴. In the context of cancer, $\beta 1$ is up-regulated in highly invasive breast carcinoma cells *in vivo* ^{5,6}, and plays crucial roles in the context of primary tumor formation and metastasis in breast, ovarian, pancreas and skin cancers ⁷⁻²¹. Further *in vitro* studies report that $\beta 1$ strongly mediates adhesion of pancreatic and ovarian cancer cells to matrix proteins including collagen 1, collagen IV, fibronectin and laminin on 2D substrates ^{7,22}, and promotes the degradation of gelatin at the whole cell level and localizes at invadopodia ²³. In addition to its effects on adhesion, knockdown of $\beta 1$ inhibits cell migration and proliferation on numerous ECM substrates ^{7,24}. Collectively, these studies suggest the importance of $\beta 1$ in mediating growth and migration in the primary tumor stroma.

The precise roles of $\beta 1$ during tumor cell extravasation, however, are less explored. Although the molecular players in extravasation (e.g. ECM molecules, endothelium) are likely similar to those in invasion and intravasation, the mechanics and sequence of the cell-cell and cell-matrix interactions are different. Furthermore, the roles and degree of requirement of specific adhesion molecules may differ depending on the context of the migration event. Thus, results obtained in these contexts may not directly translate to extravasation. In terms of metastasis, it has been shown that inhibition of $\beta 1$ significantly reduces seeding and formation of metastatic foci after several weeks, suggesting a possible defect in a preceding step of the metastatic cascade, such as extravasation ^{7,10,18,20,25,26}. However, except for a study by Stoletov et al, which demonstrated the necessity of $\beta 1$ for TEM in a zebrafish model, to our knowledge no other groups have explored in depth the role of $\beta 1$ and the associated alpha subunits in distinct steps of extravasation.²⁷ Furthermore, it remains unclear whether the defects lie in adhesion, tumor-endothelial interactions, ECM/BM interactions or even post-extravasation proliferation and survival. This is often difficult to dissect due to relatively low throughput and low spatio-temporal resolution of single cell TEM events in most *in vivo* assays.

In the present report, we utilize *in vitro* models of microvasculature to isolate and recapitulate the sequential steps in the extravasation cascade. Much is currently known about the cell adhesion molecules and proteases required by cancer cells to invade their microenvironment, but whether these same players are required for tumor cell extravasation are unclear. First, we find that $\beta 1$ expression in human tumor cells lines is necessary for efficient TEM in an *in vitro* model of human microvasculature. High-resolution imaging further reveals the requirement of activated $\beta 1$ integrin for protrusion maintenance via engagement with the sub endothelial ECM, which enables recruitment of F-actin to the

protrusion tip, followed by translocation of the cell past the endothelial layer, likely via actomyosin contractility. Specifically, adhesion onto vascular laminin via $\alpha 3\beta 1$ and $\alpha 6\beta 1$ integrins is involved in this process. Additionally, after clearing the endothelial barrier, $\beta 1$ is required for invasion past the BM. Finally, we show that $\beta 1$ depletion reduces extravasation *in vivo* and inhibits metastatic colonization, suggesting that the cumulative defects in the extravasation cascade due to $\beta 1$ depletion ultimately impairs metastasis formation.

Materials and methods

Cell culture

GFP or RFP expressing human umbilical vein endothelial cells (HUVECs) (Angioprotemie) were cultured in EGM-2MV medium (Lonza) and used at passage 4. Normal human lung fibroblasts (NHLF) (Lonza) were cultured in complete FGM (Lonza) and used between passages 4 to 8. MDA-MB-231, A-375 MA2 and 4T1 cells (parental, control and stable knockdowns) were cultured in DMEM supplemented with 10% FBS and 1% penicillin/streptomycin and 1% L-glutamate while SUM159 cells were cultured in Ham F12 supplemented with 5% FBS, 1% penicillin/streptomycin, 5 $\mu\text{g/ml}$ insulin, 1 $\mu\text{g/ml}$ Hydrocortisone, and 20ng/ml EGF. All cells were incubated at 5% CO_2 at 37°C.

DNA constructs, RNA interference and transfection

To generate miR30-based shRNAs targeting human and mouse integrins, 97-bp shRNAs were designed (Supplemental Table 1), synthesized (IDT, Coralville, Iowa) and PCR amplified to add XhoI and EcoRI sites. shRNAs were then cloned into barcoded versions of the MSCV-ZSG-2A-Puro-miR30 vector²⁸ using standard molecular biology techniques. Packaging of retrovirus and transduction of cells was done as described previously²⁹. Efficient knockdown was then confirmed using western blotting, qPCR or flow cytometry as described below. Western blots were performed as described previously²⁸ using the indicated antibodies: for immunoblots on human cells, mouse monoclonal integrin $\beta 1$ (MEM 101-A, Abcam), $\beta 3$ (Cell Signaling), GAPDH (Cell Signaling) and beta-actin (Millipore). For mouse cell lines, rabbit polyclonal anti-mouse integrin $\alpha 3$, anti-mouse integrin αV (BD Pharmigen), and mouse anti-GAPDH (Millipore) were used. Quantitative PCR (qPCR) was performed for integrin $\beta 1$ as described previously²⁸ using the MyiQ real-time PCR detection system (Bio-Rad). Flow cytometry was performed using the following primary antibodies to assess integrin surface levels: biotin conjugated anti-human $\beta 1$ integrin (P5D1, Abcam), biotin-conjugated anti-mouse integrins αV , $\beta 1$, $\beta 2$, $\beta 3$ (BD Pharmigen), or unconjugated rat anti-mouse integrin $\alpha 1$, $\alpha 2$, $\alpha 4$, $\alpha 6$, $\alpha 8$, $\beta 4$ (BD Pharmigen). Secondary antibodies were either Streptavidin-APC, or APC-conjugated anti-Rat IgG.

For siRNA-mediated knockdown of $\alpha 3$, $\alpha 6$ and $\beta 4$ integrins, cells were plated on six well plates and transfected with 25 pmol of $\alpha 3$, $\alpha 6$ or $\beta 4$ integrin Silencer Select siRNA (Thermo Fischer) using Lipofectamine RNAiMax reagent (treated twice over 48 h) before trypsinization and perfusion into microvascular networks. Knockdown was confirmed via western blotting using antibodies for $\alpha 3$ (Thermo Scientific), $\alpha 6$ (Cell Signaling) and $\beta 4$ (Cell Signaling). For visualization F-actin in transminating tumor cells, MDA-MB-231 were transduced with LifeAct mCherry (Ibidi) via standard lentiviral techniques.

Antibodies and reagents

For functional blocking of individual alpha subunits, azide-free antibodies for $\alpha 1$ (FB12), $\alpha 2$ (P1E6), $\alpha 3$ (P1B5), $\alpha 4$ (P4C2), $\alpha 5$ (P1D6), $\beta 4$ (ASC-6), $\beta 1$ (P4C10) and associated IgG₁ or IgG₃ controls from Millipore, and $\alpha 6$ (GoH3) and IgG_{2a} from Santa Cruz were incubated at 5 μ g/mL with tumor cells suspended in serum free DMEM at 0.5 million cells/mL for 30 min, prior to perfusion into microvascular devices. For neutralization of MMPs, anti-MT1-MMP catalytic domain (LEM-2/63.1, Abcam) and anti-MMP-9 (IM09-L, Calbiochem) were incubated at 15 μ g/mL with tumor cells suspended in serum free DMEM at 0.5 million cells/mL for 30 min prior to perfusion. The MMP array was from Raybiotech and used according to the manufacturer's instructions. To block laminin function, anti-laminin alpha 3 chain (P3H9-2, R&D Systems) or IgG₁ at 10 μ g/mL in EGM was perfused into the microvascular devices 10 minutes prior to tumor perfusion.

Immunofluorescence and imaging analysis

Devices were fixed with 4% paraformaldehyde for 10 min, permeabilized with 0.1% Triton-X and then blocked with 10% BSA and 1% goat serum in PBS for 2 h. Samples were incubated in primary antibodies against human CD31, vinculin at 1:100 (Sigma Aldrich), human Tks-5 at 1:50 (Santa Cruz), human collagen IV, laminin, fibronectin, or $\beta 1$ integrin activated conformation (clone 12G10) at 1:100 (from Abcam) overnight in blocking buffer at 4°C. After washing, devices were incubated with secondary antibody (Alexa Fluor 568 goat anti-mouse or 568 goat anti-rabbit) at 1:200, DAPI at 1:1000, and Alexa Fluor 647 phalloidin (all from Invitrogen) for 4 h.

Lungs were processed and stained as previously described³⁰. Briefly, lobes were cut into smaller pieces and blocked for 1 h (10% goat serum and 0.3% Triton-X), followed by incubation in mouse anti-CD 31 (BD Biosciences) at 1:100 overnight at 4°C. Lungs were washed in wash buffer and incubated in secondary antibody (Alexa Fluor 568 goat anti-rat, Invitrogen) at 1:500 overnight at 4°C.

Microfluidics-based microvascular network extravasation assay

A microfluidics-based cell culture system capable of generating perfusable microvascular networks was used in this study, similar to that described previously³¹, with some modifications. Microfluidic device fabrication is outlined in detail elsewhere³². The platform features three independent hydrogel regions (1300 μ m wide by 110 μ m high by 0.8 cm long) separated by media channels (SI Fig. 1A). ECM hydrogels are held in place via the surface tension generated in the presence of small trapezoidal microposts³³. To form vascular networks, HUVECs and NHLFs were suspended separately at final concentrations of 5×10^6 /mL and 4×10^6 /mL respectively, in 2.5 mg/mL fibrinogen (Sigma) and 0.25 U/mL thrombin (Sigma) solutions. Tumor cells are introduced into the microvascular networks on day 4 of device culture, after which they were transferred to a confocal microscope (Olympus FV1000) equipped with an environmental chamber for imaging of extravasation events.

Microfluidics-based vertical endothelial monolayer extravasation assay

In some experiments, a microfluidics-based endothelial monolayer was used in place of microvascular networks to achieve visualization at greater spatial resolution of single cell extravasation events, due to its planar configuration³⁴. Here, a single lumen is modeled by forming an intact monolayer on the hydrogel and micro-post surfaces (SI Fig. 1A). Briefly, a type 1 rat-tail collagen and fibrinogen were prepared obtain a final gel concentration of 2.5 mg/mL fibrin and 0.24 mg/mL collagen I mixture and injected. HUVECs suspended at 2.5×10^6 /mL in EGM-2MV were then seeded into the media regions and cultured for 48 h at 37°C and 5% CO₂ until a confluent monolayer was formed on the gel-media interface. Tumor cells at 0.1 million cells/mL were perfused into one media channel. Devices were tilted at a 90-degree angle at 37°C for 30 min in a humidified chamber.

Adhesion assay

To test the degree of tumor-endothelial adhesion without the added factor of physical trapping, rectangular PDMS micro-channels were fabricated (0.3 cm wide by 110 μ m high by 5 cm long). Three inlet holes were punched (two on both ends and one in the middle). HUVECs (2 million cells/mL) were seeded into micro-channels. At the formation of a confluent monolayer, tumor cells at 1 million cells/mL in serum-free endothelial basal medium (EBM) were perfused from the outer inlet port (while keeping the center port plugged) and allowed to settle and adhere 10, 30 or 60 min. EBM is then perfused into the middle port via a syringe pump to obtain a shear rate of 5 dynes/cm² for 15 min, after which tumor cells are recounted.

***In vivo* mouse extravasation assay**

One hundred microliters of cell suspension in PBS (0.5 million cells) were injected via lateral tail vein of female NOD/SCID/gamma mice. Mice were euthanized and lungs were collected after inflation with 4% formaldehyde, 0.3% Triton X-100 at 3, 16 and 24 h.

***In vivo* metastasis assay**

miR-30 based shRNAs targeting each integrin subunit were designed and cloned into uniquely barcoded versions of the MSCV-ZSG-2A-Puro-miR30 vector²⁸ as described above, and then used to stably transduce 4T1 cells. Once integrin knockdown was confirmed via FACs, individual 4T1 cell populations were mixed in equal numbers and injected into the lateral tail veins of mice. Lungs were isolated for analysis after 17 days. A starting population was also collected at the time the mixed cell populations were injected and was used for normalization of subsequent samples. Luminex-based analysis of metastasis burden was performed as described previously²⁸. Briefly, genomic DNA was isolated from lungs and starting cell pellets and barcodes were PCR-amplified using biotinylated primers that bind to common regions in the vector that flank the DNA barcode. PCR product was then quantified by the Genetic Analysis Platform at the Broad Institute (Cambridge, MA) using Luminex technology. For this, PCR product was hybridized to uniquely dyed Xmap beads (Luminex Corporation) that were precoupled to oligonucleotide sequences complementary to the 21-nt barcodes contained in our vectors. Barcodes were then quantified by incubating the beads with streptavidin-conjugated allophycocyanin (APC) and measuring the APC

signal on each bead using the Luminex FlexMap 3D system (Luminex Corporation). The relative amounts of each unique barcode in each lung sample were calculated from the raw APC signals. This was performed by normalizing the signal for each unique barcode to the signal for the same barcode in the starting population.

Quantification of extravasation and statistics

In all *in vitro* experiments (unless otherwise indicated), the average TEM efficiency is the average of the mean of 3 devices per condition and 3 independent experiments (total 9 devices). The value of each device was calculated as an average of 6 fields of view (microvascular networks) or 10 fields of view (monolayer device). Statistical analysis was performed with SigmaPlot using Student's two-tailed *t*-test when comparing two conditions, or ANOVA with Tukey's post-hoc analysis when applicable. Unless otherwise indicated, "n" represents one independent experiment with at least 3 devices per condition.

Results

$\beta 1$ integrins are required for efficient transendothelial migration from *in vitro* microvascular networks and *in vivo* mouse lung extravasation assays

To investigate the importance of integrin $\beta 1$ in the extravasation, we employ a 3D microfluidic model of human microvascular networks previously developed by our group (Fig. 1A, SI 1A). The interconnected lumens formed via a vasculogenic-like process recapitulate the microcirculation in which tumor cells arrest due to size restriction and/or adhesion and extravasate, thereby exhibiting greater physiological relevance than most *in vitro* assays, in terms of geometry and barrier function. Tumor cells can be perfused into the microvessels and extravasation events can be monitored dynamically. Importantly, the assay allows significantly clearer real-time visualization of TEM on a single-cell level, compared to most *in vivo* and *in vitro* techniques. Lumens lie largely in the same plane, allowing intravascular, partially transmigrated and fully transmigrated cells to be clearly differentiated even at low magnifications (i.e. 10 to 20X) (Fig. 1D).

We stably expressed shRNAs targeting either control firefly luciferase (control) or integrin $\beta 1$ (*$\beta 1$ KD*) in human metastatic human breast cancer (MDA-MB-231, SUM-159), highly metastatic human melanoma (A-375 MA2) and mouse mammary carcinoma (4T1) cell lines. Silencing was verified via western blotting (Fig. 1B, SI Fig. 2A), flow cytometry, and qPCR (Fig. SI 2B). Cells were perfused into *in vitro* microvascular networks and TEM events were tracked via live confocal microscopy (SI Movie 1). Reduction of $\beta 1$ via shRNA and blocking antibodies in MDA-MB-231 significantly abrogated TEM in microdevices at 6 h, while knockdown of $\beta 3$ integrin had no significant effects, indicating that the observed attenuation of TEM may be specific to $\beta 1$ (Fig. 1C). In our assays, transmigration is defined as fully clearing the endothelial barrier. The *$\beta 1$ -4* shRNA, with an intermediate level of knockdown (66% mRNA inhibition), exhibited an intermediate TEM rate at 6 h, suggesting a graded response with decreasing $\beta 1$ expression (Fig. SI 2C). Longer-term kinetics of transmigration were tested in all cell lines revealing that the decrease in TEM due to $\beta 1$ knockdown is likely not cell line specific. Furthermore, TEM rates reach a plateau at ~ 12 h in both control and *$\beta 1$ KD* conditions (Fig. 1E), indicating that the defects in transmigration are not simply due

to a delay in the progression of extravasation. Additionally, proliferation assays reveal no significant differences between control and $\beta 1$ KD cells in the span of 48 h (Fig. SI 2D), thus the number of TEM events is likely not influenced by differences in cell proliferation throughout the duration of the transmigration assay.

To validate our findings in an *in vivo* context, MDA-MB-231 control and $\beta 1$ KD cells were injected into Nod/Scid/gamma mice via the lateral tail vein. Close inspection via confocal microscopy and 3D rendering at 60X allowed visualization of individual tumor cells near the tissue surface (Fig. 1F, Fig. SI 3A). Tumor cells surrounded by a continuous and distinct border of CD31 staining were scored as intravascular, while all other cells were counted as transmigrated, even if partly surrounded by vascular staining. Both control and $\beta 1$ KD cells were mainly contained within blood vessels at 3 h post injection. At 16 h there was a significant (~5 fold) difference in the number of transmigrated control cells versus $\beta 1$ KD, with the difference increasing at 24 h (Fig. 1G).

Combined, these results confirm that tumor integrin $\beta 1$ is essential for TEM. However, the role of $\beta 1$ in other distinct steps of extravasation (Fig. 2A) both preceding and subsequent to TEM remains unclear. These steps include tumor-endothelial adhesion, tumor cell protrusion initiation and formation into the sub-endothelial matrix, interaction with the endothelial BM, and migration through the parenchyma. Due to the challenges associated high resolution and dynamic imaging *in vivo*, we capitalized on the unique capabilities of our *in vitro* microvasculature assay.

$\beta 1$ integrin does not mediate adhesion to endothelium but adhesion to sub-endothelial matrix, under flow conditions

We further investigated whether $\beta 1$ integrin plays a role in heterotypic endothelial-tumor adhesion, a possible precursor to TEM. It is believed that since tumor cells that are rapidly cleared from the circulation *in vivo*, cells that quickly arrest in the vasculature and extravasate may have a selective advantage toward establishing new colonies^{26,35}.

To isolate the effect of adhesion, tumor cells were seeded into endothelial-lined chambers and allowed to settle and adhere for 10, 30 or 60 min. This is followed by continuous perfusion of media for 15 min at 5 dynes/cm². With 30 or 60 min of settling time, more control cells remained adherent than $\beta 1$ KD cells post-perfusion, with the greatest difference being at 60 min (Fig. SI 4A). In contrast, 10 min of settling time prior to perfusion resulted in no significant differences. Upon closer inspection, more than half of all adherent cells in 30 or 60 min control samples had gained access to the subendothelial ECM, as identified by short (1–4 μ m) tumor cell protrusions extending past the plane of the endothelium (Fig. SI 4A–B). In contrast, the few adherent $\beta 1$ KD cells did not exhibit protrusions. This suggests that $\beta 1$ mediates adhesion to the underlying matrix, rather than the endothelium, thereby providing the force necessary to resist detachment under flow. We also note that adherent cells at the 10 min time point do not exhibit discernable protrusions, suggesting that early tumor-endothelial adhesion exists, but is likely mediated by other adhesion molecules such as selectins (CD62) or glycoproteins like CD44³⁶, rather than integrins.

In vivo, we observed similar numbers of control and $\beta 1$ KD cells in lungs at early time points (3 and 16 h post-injection) and only a slight difference at 24 h (Fig. SI 4C). This lack of $\beta 1$ dependence compared to *in vitro* findings could be due to a tendency for physical trapping to dominate over adherence *in vivo*, since narrow capillaries are not recapitulated in the *in vitro* flow channel. That is, while we find that $\beta 1$ can mediate adhesion under flow due to subendothelial matrix anchorage, physical trapping of cells may be the rate-controlling factor in retention *in vivo*.

Activated $\beta 1$ and actin-rich protrusion formation precede and are required for complete transmigration

Previously, it has been suggested that tumor cells form invadopodia-type processes past the endothelium^{37,38} and that abrogating these structures prevents extravasation in chick chorioallantoic membrane assays (CAM)³⁸. Thus, we sought to understand the role of $\beta 1$ in protrusion formation and endothelial barrier breaching. We employ an alternate “vertical monolayer device” consisting of microchannels connected by 3D ECM hydrogels, where tumor cells are seeded in one channel, arrest onto and extravasate across an endothelial monolayer into a fibrin-type 1 collagen matrix^{34,39}. In this assay, migration across and through the monolayer and subendothelial matrix occurs in the plane of view; thus, protrusion formation and dynamics during extravasation can be observed in high detail (Fig. SI 1B, SI 5A–C). Time-lapse confocal images taken over 6 h reveal that transmigrating control cells extend numerous thin filipodial-like protrusions past a gap in the endothelial barrier as early as 20 min post-perfusion (Fig. 2B). In contrast, $\beta 1$ KD cells remained largely spherical and lacked protrusions in nearly all cells sampled (Fig. 2C). Surprisingly, while $\beta 1$ KD tumor cells do not transmigrate, there is still discernable endothelial gap formation at the site of tumor arrest, suggesting that $\beta 1$ does not significantly hinder the ability for endothelial disruption (Fig. SI 5D).

Immunostaining for the active conformation of $\beta 1$ showed localized punctates at the tips of the protrusions extending into the sub-endothelial matrix in transmigrating control cells only (Fig. 2F), suggesting that $\beta 1$ mediated protrusion formation and ECM engagement is required for complete TEM. Dynamic tracking of tumor cell protrusions embedded in 3D collagen 1-fibrin mixed matrices reveal that control cells quickly extend protrusions that often persist (>30 min), and subsequently take on an elongated morphology. In contrast, $\beta 1$ KD cells exhibit small, short-lived transient protrusions and typically retain a more spherical shape (Fig. SI 6A–B). Thus, it is likely that $\beta 1$ is not required for protrusion initiation, but for protrusion stabilization via $\beta 1$ mediated anchorage onto vascular BM; this is supported by previous findings but in a 2D context²³. Furthermore, live time-lapse imaging of tumor F-actin during TEM reveals actin-rich punctates at the tips of protrusions extending past the endothelium (Fig. 2G). At times, these actin-rich protrusions are also diffusely marked by the focal adhesion protein vinculin (Fig. 2H), which is generally diffuse in tumor cells embedded in 3D collagen gels (data not shown). There has recently been growing evidence that integrins play important roles in invadopodia formation and function, in particular $\alpha 1\beta 3$ and $\beta 1$ integrins; however, whether invadopodia form during extravasation is unclear. Indeed immunofluorescent imaging showed Tks5 punctates specifically in protrusions, suggesting the presence of functional and degradatory invadopodia during TEM.

Together our results suggest that $\beta 1$ mediates tumor cell protrusion stabilization by facilitating anchorage vascular BM, followed by recruitment of actin and possibly focal adhesion proteins, at the protruding-edge. Subsequent actomyosin-mediated contractions then likely pull the remaining cell body past the endothelium.

$\beta 1$ integrins mediate invasion across the basement membrane

Upon closer inspection of fixed images in both microvascular network and monolayer assays, fully transmigrated cells were observed in 3 distinct “positions” relative to the endothelium: (1) directly adjacent to the abluminal surface, (2) adjacent but elongated perpendicular to the lumen, and (3) migrated away from the abluminal surface. At 4 h control cells were found in all three positions while of the few (<6%) $\beta 1$ KD cells that had transmigrated, almost all were exclusively confined to “position 1” (Fig. 3A). Not only were transmigration distances significantly reduced in knockdown cells, few protrusions were observed (Fig. 3B), consistent with their rounded and non-protrusive morphology.

Since $\beta 1$ KDs are unable to migrate away from the endothelium, we hypothesized that tumor cells were unable to invade past the endothelium BM. This could be due to the inability to attach to and/or degrade the underlying matrix proteins. During the formation of microvasculature, endothelial cells forming the *in vitro* microvessels deposit a continuous layer of BM proteins including collagen IV, laminin and fibronectin (Fig. SI 7A) similar to *in vivo* vasculature. Staining for laminin revealed tumor cells in four “states” relative to the BM and endothelium: (1) breaching the endothelium but not the BM, (2) fully transmigrated but intercalated between the endothelium and BM, (3) breaching the BM, and (4) completely cleared of endothelium and BM (Fig. 3C). Devices immunostained at 2 h revealed that out of the subpopulation of transendothelial migrating cells, both control and $\beta 1$ KD cells were mostly found in state (1) where the endothelium had been breached but not the laminin layer. Subsequently, devices fixed at 9 h showed that most transmigrating control cells were in states (3) and (4), breaching both the endothelium and laminin (Fig. 3D). This suggests that the formation of stable protrusions requires adhesive interactions with the underlying BM, which is then followed by degradation and invasion past it. Conversely, nearly all transmigrating $\beta 1$ KD cells remained in state (1). Similar results were found in the vertical monolayer assay when immunostained for collagen IV (SI Fig. 7 B–D).

Due to the inability of $\beta 1$ KD cells to invade past the BM, we hypothesized that MMPs are required to digest BM proteins, and that $\beta 1$ KD cells may exhibit a defect in MMP activity. We tested the effect of anti-MT1-MMP and anti-MMP-9 (two major MMPs implicated in BM/laminin degradation) on TEM efficiency in microvascular networks at 6 h. Both anti-MT1-MMP and anti-MMP-9 slightly reduce TEM efficiency ($p=0.046$ and $p=0.089$, respectively) (although not comparable to knocking down $\beta 1$ integrins) suggesting that initial crossing of the EC barrier is only weakly dependent on these proteases (Fig. SI 7E). Further immunostaining for laminin on the same devices revealed that transmigrating cells treated with either anti-MT1-MMP anti-MMP-9 were both less likely to breach the laminin layer upon exiting the endothelium compared to control cells at the same time point ($p=0.026$ and $p=0.008$, respectively). Together this suggests that MT1-MMP and MMP-9 are involved in matrix degradation once the cell has transmigrated, while playing a smaller role

in the initial crossing of the endothelium. However, when MMP secretion levels were tested via an MMP antibody array, no discernable differences were found between $\beta 1$ KD and control shRNA MDA-MB-231 in secreted levels of MMP-1, 2, 3, 8, 9, 10 and TIMP-1, 2, and 4. Further testing of MMP-9 and MMP-2 levels via zymography also revealed no differences (data not shown). Despite these results, we cannot completely rule out the possibility of $\beta 1$ KD-induced defects in MMP localization and/or activation in the specific context of TEM, since conventional conditioned medium collection techniques (cells mono-cultured on a 2-D culture dish) do not recapitulate the specific context of TEM and MMP localization.

Transendothelial migration is mediated by $\beta 3\beta 1$ and $\beta 6\beta 1$ integrins via interactions with sub-endothelial laminin

Our results suggest that TEM is facilitated by the formation of activated $\beta 1$ and actin-rich protrusions, which then form stable adhesions onto the subendothelial matrix, and likely followed by contraction at the protruding edge. Because we demonstrated that tumor cell protrusions associate closely with the BM during the initial hours of TEM (Fig. 3C), we hypothesized that the defects induced by $\beta 1$ depletion are partly due to the inability of protrusions to bind to specific underlying BM proteins. To determine which alpha subunits and corresponding ECM ligands are important for TEM, we first employed function blocking antibodies for integrins $\alpha 1$, 2, 3, 4, 5, 6, v, $\beta 1$ and $\beta 4$ to tumor cells prior to, and during the *in vitro* microvasculature assay. Reduction of integrin(s) function was verified via adhesion assays to collagen I, collagen IV, fibronectin and laminin (SI Fig. 8A). At 6 h post tumor cell seeding, TEM rates for most individually blocked alpha subunits ($\alpha 1$, 2, 3, 4 and 5) and $\beta 4$ were not significantly different, while there were slight attenuations when $\alpha 6$ and αv were blocked, and when $\alpha v/\alpha 5$ and $\alpha 1/\alpha 2$ were co-blocked (Fig. 4A). The most striking decrease occurred when laminin-binding integrins $\alpha 3$ and $\alpha 6$ were co-blocked ($p=0.0059$), indicating that adhesion to subendothelial laminin is critical for efficient TEM. This also suggests that sub-endothelial fibronectin and collagen-mediated adhesion through integrins $\alpha v/\alpha 5$ and $\alpha 1/\alpha 2$, respectively may not be a major factor in TEM. We further tested endothelial permeability in the presence of each blocking antibody at 6 h and found that barrier function was not impaired in this time frame (data not shown). To further confirm our results, we silenced $\alpha 3$ and $\alpha 6$ via siRNA (Fig. 4B) and carried out longer-term (~24 h) kinetics experiments. This also determines whether the defect in TEM is due to a delay in extravasation. At 24 h post tumor seeding, co-silencing of $\alpha 3$ and $\alpha 6$ continues to yield a significantly lower TEM rate compared to silencing $\alpha 3$ or $\alpha 6$ alone, suggesting that the reduction of one laminin binding integrin may be compensated by the other (Fig. 4C). Furthermore, silencing of $\beta 4$ integrin did not result in significant changes in TEM over 24 h, indicating that $\alpha 6\beta 1$, and not $\alpha 6\beta 4$ (which also bind to laminin), is likely at play (SI Fig. 8B).

Dynamic tracking of TEM on individual tumor cells revealed that the time required to reach a state of discernable stable protrusion formation past the endothelium was longer in $\alpha 3/\alpha 6$ co-knockdown cells compared to controls (SI Fig. 8C). Furthermore, blocking of microvascular devices with anti-laminin antibodies prior to tumor cell perfusion resulted in a significantly lower percentage of cells exhibiting protrusions at early time points of 1 and 4

h, strongly suggesting that the ability to adhere to BM laminin is important in the specific context of extravasation (Fig. 8D). However, while co-blocking $\alpha 3$ and $\alpha 6$ significantly decreases TEM efficiency, it does not reach the levels associated with blocking $\beta 1$. Combined with the finding that blocking of most individual alpha subunits only yields small or insignificant changes, it is highly likely that multiple alpha subunits function simultaneously to facilitate TEM.

$\beta 1$ integrin is required for metastatic colony formation *in vivo*

Our results show that loss of $\beta 1$ integrins significantly impairs tumor cell extravasation by influencing multiple processes during extravasation, which is widely believed to be a rate-limiting step in metastatic colonization of distant organs. Therefore, we tested whether $\beta 1$ knockdown impairs metastatic colonization. Since several cell types in the immune system are known to influence metastatic colonization^{40,41}, we performed these experiments using the highly metastatic mouse mammary carcinoma cell line 4T1 which is syngeneic in Balb/C mice. These 4T1 $\beta 1$ KDs were confirmed to impair extravasation in our microvascular network assay (Fig. 1E).

To test the effect of knocking down individual integrin subunits, we utilized a previously developed a Luminex-based, multiplexed assay for metastatic colonization (Fig. 5A)²⁸. 4T1 cells stably expressing uniquely DNA-barcoded vectors with shRNAs targeting each integrin subunit were individually generated and efficient knockdown of each integrin subunit was confirmed by flow cytometry (Supplementary Table 2). These cell lines were then mixed in equal numbers and utilized for multiplexed tail vein metastasis assays. Cell lines expressing shRNAs that inhibit metastatic colonization will be significantly depleted in lungs of these mice relative to control shRNAs. Cells expressing shRNAs targeting integrin $\beta 1$ were significantly reduced in the lungs relative to control shRNAs (Fig. 5B), indicating the loss of $\beta 1$ significantly impairs metastatic colonization. In contrast, targeting other beta subunits or individual alpha subunits did not significantly reduced in the lungs relative to control shRNAs, suggesting that the functions of individual alpha subunits are dispensable for metastatic colonization. This finding is consistent with the earlier results presented, showing that blocking of individual alphas and other beta subunits does not significantly impair TEM in *in vitro* microvasculature (Fig 1B, Fig. 4). Together these findings suggest that the ability to successfully extravasate is strongly correlated with the ability to form metastasis, and that $\beta 1$ integrin is required for metastatic formation.

Discussion

Tumor cell extravasation is a key step during cancer metastasis, yet the precise mechanisms that regulate this process remain unclear. This is partly due to the difficulty of most *in vivo* assays in isolating the effect of different perturbations on discrete steps during extravasation. Furthermore, *in vivo* models are often hindered by relatively low spatio-temporal resolution of extravasation events and the tortuosity of *in vivo* vasculature presents challenges in scoring extravascular and intravascular cells, rendering the analysis subjective. To address this need, we have recently developed *in vitro* microvascular platforms capable of observing multiple steps of the extravasation cascade in high detail, where vessels largely lie in the

same plane of view and distances between the cells and microscope objective is <300 microns. This assay also features increased physiological relevance in terms of geometry and barrier function than most *in vitro* platforms. Thus, despite the essential role that *in vivo* extravasation models play in recapitulating physiological conditions, the *in vitro* assays used in this study are more suitable for discerning the spatial organization of tumor-endothelial cell interactions. Using our assays, we are able to pinpoint the distinct roles of tumor $\beta 1$ integrin in tumor-endothelial and tumor-BM interactions during extravasation. First, $\beta 1$ integrin is activated at the tip of leading protrusions penetrating the endothelium, allowing adhesion to subendothelial ECM, in particular, BM laminin via $\alpha 3\beta 1$ and $\alpha 6\beta 1$ integrins. Engagement of these integrins with their ligand allows stabilization and growth of these protrusions, which is followed by recruitment of F-actin at the protruding edge. This then enables the cell to translocate by pulling itself past the gap formed in the endothelium (Fig. 6).

The lack of discernable tumor cell protrusions during transmigration in $\beta 1$ KD cells suggests that the extension of cytoplasmic projections is required for complete extravasation. Cells transmigrating in our microvascular networks exhibit invadopodial-like extensions into the sub endothelial matrix during transmigration. Furthermore, these protrusions are marked by co-localized punctate regions of F-actin, activated $\beta 1$ integrin, vinculin and Tks5 at the tips of the protrusion. In contrast, these proteins are only weakly diffuse in the intravascular portion of transmigrating cells, as well as in non-transmigrating cells. In support of this, it has been shown that invadopodia formation is associated with $\beta 1$ and $\beta 3$ integrins⁴², and that pharmacological inhibition of invadopodia maturation (Tks5) and function (Tks4) results in an abrogation of extravasation in CAM models and metastatic colony formation *in vivo*³⁸. During the initial stages of TEM (20 min to 1 h) tumor cells begin by extending small actin rich protrusions (~1–3 μm deep) into the extravascular space. Combined with the observation that these initial protrusions do not breach but rather associate closely with the subendothelial BM, we hypothesized that $\beta 1$ integrins facilitate the engagement of these protrusions to specific underlying BM proteins via specific alpha integrin subunits. In support of this, *in vivo* studies have shown that tumor cells extend processes past the endothelium, contacting the basal lamina^{43–45}. The integrin profile of MDA-MB-231 has previously been characterized and shown to express a variety of alpha subunits (including $\alpha 1$ to $\alpha 6$ and ν)⁴⁶, however whether all or only a specific subset of these are required in extravasation is unclear. Numerous studies have demonstrated the importance of various alpha integrins in the context of 3D invasion and contribution to metastatic formation^{10,14,17,21,22,26,47}. However, while similar ECM components may be present in both the primary site and extravasation microenvironments, their spatial distributions and abundance may differ. Additionally, the necessity of engagement to specific ECM components may also differ depending on the context of migration. Using our assays, we find that co-knockdown of $\alpha 3$ and $\alpha 6$ integrins results in the most significant defect in TEM, indicating that adhesion to BM laminin is required in the context of TEM, and likely facilitates maintenance of tumor cell projections past the endothelium. In fact, it has been found that the ability to adhere onto vascular laminin may be involved in the extravasation step, which is suggested by the requirement of $\alpha 3\beta 1$ for adhesion to exposed regions of pulmonary vascular LN-5 and subsequent metastatic foci formation in a mouse model²⁶. In

support of this, our dynamic imaging reveals co-blocking $\alpha 3$ and $\alpha 6$ integrins results in a slower rate of protrusion formation into the subendothelial matrix. In an *in vivo* context, it may be advantageous for tumor cells to form stable anchorage into the matrix faster, in order to gain better chances of escaping the hostile intravascular environment. In contrast, blocking integrin receptors αv and $\alpha 5$ for fibronectin do not yield significant results, despite the fact that fibronectin is present on the abluminal surface of the vessels. This further suggests that the inability to adhere to laminin cannot be fully compensated via adhesion to other available ECMs during extravasation.

The BM scaffold is a tight covalently cross-linked mesh formed by laminin and type IV collagen that is bridged by nidogens on which other components are bound. It seems highly unlikely that a cell could squeeze through pores on the order of 50 nm; however, tumor cells constantly migrate across basement membranes⁴⁸. Thus, the process has long been thought to require local degradation of the BM with matrix metalloproteinases (especially MT-MMPs), which may be recruited via integrin engagement to the ECM. These proteases are well characterized in the context of invasion, but whether the same factors are involved in vascular BM invasion are largely unclear. Because we observe the inability of $\beta 1$ KDs to migrate away from the endothelium post-transmigration, we hypothesized that $\beta 1$ mediates the localization and production of MMPs that are required to degrade the vascular BM. In support of this hypothesis, studies show that $\beta 1$ is required for invadopodia formation and matrix degradation in both 2D and 3D ECM scenarios^{49,50,23}. Indeed, immunostaining of laminin in our devices revealed that while control cells begin to breach the laminin layer within the first 6 to 9 h of TEM, few transmigrating $\beta 1$ KD cells were able to invade the laminin layer, remaining trapped between the endothelium and BM. Furthermore, blocking of MMP-9 and MT1-MMP phenocopied this behavior, suggesting that localization and activation of MMPs are involved in BM breaching.

In vivo metastasis assays show a clear role of $\beta 1$ in dissemination^{7,10,17,18,20,25,26} (Fig. 5); however, whether and how the defects lie in extravasation or even post-extravasation micro-metastatic growth remained unclear. In this report, we demonstrate that the tumor $\beta 1$ subunit is an indispensable player in the tumor cell extravasation cascade, and that its depletion contributes to an overall decrease in formation of metastases *in vivo*. Using high-resolution *in vitro* assays, we find that tumor cells first send activated $\beta 1$ -rich protrusions past the endothelium, which engages with subendothelial matrix, in particular laminin, via $\alpha 3\beta 1$ and $\alpha 6\beta 1$ integrins. This is followed by protrusion stabilization, F-actin recruitment, translocation of the tumor cell into the parenchyma, and subsequently, $\beta 1$ -mediated invasion past the vascular basement membrane.

Supplementary Material

Refer to Web version on PubMed Central for supplementary material.

Acknowledgments

This work was supported by the NCI grant (U01: 1U01CA202177-01; to RDK) and the National Science Foundation (NSF GRFP: to MBC).

References

1. Heyder C, et al. Realtime visualization of tumor cell/endothelial cell interactions during transmigration across the endothelial barrier. *J Cancer Res Clin Oncol*. 2002; 128:533–8. [PubMed: 12384796]
2. Haier J. An Intravital Model to Monitor Steps of Metastatic Tumor Cell Adhesion Within the Hepatic Microcirculation. *J Gastrointest Surg*. 2003; 7:507–515. [PubMed: 12763408]
3. Ganguly KK, Pal S, Moulik S, Chatterjee A. Integrins and metastasis. 2013:251–261.
4. Hynes RO. Integrins: Bidirectional , Allosteric Signaling Machines In their roles as major adhesion receptors , integrins. 2002; 110:673–687.
5. Orini MM, et al. THE $\alpha 3 \beta 1$ INTEGRIN IS ASSOCIATED WITH MAMMARY CARCINOMA CELL METASTASIS , INVASION , AND GELATINASE B (MMP-9) ACTIVITY. 2000; 342:336–342.
6. Trikha M, De Clerck YA, Markland FS. Metastatic a Snake Venom Disintegrin. Inhibits 1J @ Cell Adhesion and Blocks Experimental Human Melanoma. 1994:4993–4998.
7. Grzesiak JJ, et al. Knockdown of the $\beta(1)$ integrin subunit reduces primary tumor growth and inhibits pancreatic cancer metastasis. *Int J Cancer*. 2011; 129:2905–15. [PubMed: 21491421]
8. Lahlou H, Muller WJ. B1-Integrins Signaling and Mammary Tumor Progression in Transgenic Mouse Models: Implications for Human Breast Cancer. *Breast Cancer Res*. 2011; 13:229. [PubMed: 22264244]
9. Huck L, Pontier SM, Zuo DM, Muller W. J beta1-integrin is dispensable for the induction of ErbB2 mammary tumors but plays a critical role in the metastatic phase of tumor progression. *Proc Natl Acad Sci U S A*. 2010; 107:15559–64. [PubMed: 20713705]
10. Mitra, aK, et al. Ligand-independent activation of c-Met by fibronectin and $\alpha(5)\beta(1)$ -integrin regulates ovarian cancer invasion and metastasis. *Oncogene*. 2011; 30:1566–76. [PubMed: 21119598]
11. White DE, et al. Targeted disruption of $\beta 1$ -integrin in a transgenic mouse model of human breast cancer reveals an essential role in mammary tumor induction. 2004; 6:159–170.
12. Weaver VM, et al. Reversion of the Malignant Phenotype of Human Breast Cells in Three-Dimensional Culture and In Vivo by Integrin Blocking Antibodies. 1997; 137:231–245.
13. Liu Y, et al. Cleaved high-molecular-weight kininogen and its domain 5 inhibit migration and invasion of human prostate cancer cells through the epidermal growth factor receptor pathway. *Oncogene*. 2009; 28:2756–65. [PubMed: 19483730]
14. Yoshimura K, et al. Integrin alpha2 mediates selective metastasis to the liver. *Cancer Res*. 2009; 69:7320–8. [PubMed: 19738067]
15. Ramirez NE, et al. The $\alpha 2 \beta 1$ integrin is a metastasis suppressor in mouse models and human cancer. 2011:121.
16. Brakebusch C, et al. b 1 integrin promotes but is not essential for metastasis of ras-myc transformed @ broblasts. 1999; 1:3852–3861.
17. Zhou B, et al. Integrin $\alpha 3 \beta 1$ can function to promote spontaneous metastasis and lung colonization of invasive breast carcinoma. *Mol Cancer Res*. 2014; 12:143–54. [PubMed: 24002891]
18. Qian F, Zhang ZC, Wu XF, Li YP, Xu Q. Interaction between integrin alpha(5) and fibronectin is required for metastasis of B16F10 melanoma cells. *Biochem Biophys Res Commun*. 2005; 333:1269–75. [PubMed: 15979576]
19. Felding-habermann B. Integrin adhesion receptors in tumor metastasis. 2003:203–213.
20. Reticker-Flynn NE, et al. A combinatorial extracellular matrix platform identifies cell-extracellular matrix interactions that correlate with metastasis. *Nat Commun*. 2012; 3:1122. [PubMed: 23047680]
21. Desgrosellier JS, Cheresh Da. Integrins in cancer: biological implications and therapeutic opportunities. *Nat Rev Cancer*. 2010; 10:9–22. [PubMed: 20029421]
22. Ahmed N, Riley C, Rice G, Quinn M. Role of integrin receptors for fibronectin, collagen and laminin in the regulation of ovarian carcinoma functions in response to a matrix microenvironment. *Clin Exp Metastasis*. 2005; 22:391–402. [PubMed: 16283482]

23. Beaty BT, et al. β 1 integrin regulates Arg to promote invadopodial maturation and matrix degradation. *Mol Biol Cell*. 2013; 24:1661–75. S1–11. [PubMed: 23552693]
24. Shibue T, Weinberg RA. Integrin β 1 -focal adhesion kinase signaling directs the proliferation of metastatic cancer cells. 2009:106.
25. Wang D, et al. The pivotal role of integrin β 1 in metastasis of head and neck squamous cell carcinoma. *Clin Cancer Res*. 2012; 18:4589–99. [PubMed: 22829201]
26. Wang H, et al. Tumor cell α 3 β 1 integrin and vascular laminin-5 mediate pulmonary arrest and metastasis. *J Cell Biol*. 2004; 164:935–41. [PubMed: 15024036]
27. Stoletov K, et al. Visualizing extravasation dynamics of metastatic tumor cells. *J Cell Sci*. 2010; 123:2332–41. [PubMed: 20530574]
28. Lamar JM, et al. The Hippo pathway target, YAP, promotes metastasis through its TEAD-interaction domain. *Proc Natl Acad Sci*. 2012; 109:E2441–E2450. [PubMed: 22891335]
29. Stern P, et al. A system for Cre-regulated RNA interference in vivo. *Proc Natl Acad Sci U S A*. 2008; 105:13895–900. [PubMed: 18779577]
30. Labelle M, Begum S, Hynes RO. Platelets guide the formation of early metastatic niches. *Proc Natl Acad Sci U S A*. 2014; 111:E3053–61. [PubMed: 25024172]
31. Chen MB, Whisler JA, Jeon JS, Kamm RD. Mechanisms of tumor cell extravasation in an in vitro microvascular network platform. *Integr Biol*. 2013; 5:1262–1271.
32. Shin Y, et al. Microfluidic assay for simultaneous culture of multiple cell types on surfaces or within hydrogels. *Nat Protoc*. 2012; 7:1247–59. [PubMed: 22678430]
33. Whisler, Ja; Chen, MB.; Kamm, RD. Control of perfusable microvascular network morphology using a multiculture microfluidic system. *Tissue Eng Part C Methods*. 2014; 20:543–52. [PubMed: 24151838]
34. Zervantonakis IK, et al. Three-dimensional microfluidic model for tumor cell intravasation and endothelial barrier function. *Proc Natl Acad Sci U S A*. 2012; 109:13515–20. [PubMed: 22869695]
35. Labelle M, Begum S, Hynes RO. Direct signaling between platelets and cancer cells induces an epithelial-mesenchymal-like transition and promotes metastasis. *Cancer Cell*. 2011; 20:576–90. [PubMed: 22094253]
36. Reymond N, D'Água BB, Ridley AJ. Crossing the endothelial barrier during metastasis. *Nat Rev Cancer*. 2013; 13:858–70. [PubMed: 24263189]
37. Chen MB, Whisler Ja, Jeon JS, Kamm RD. Mechanisms of tumor cell extravasation in an in vitro microvascular network platform. *Integr Biol (Camb)*. 2013; 5:1262–71. [PubMed: 23995847]
38. Leong HS, et al. Invadopodia are required for cancer cell extravasation and are a therapeutic target for metastasis. *Cell Rep*. 2014; 8:1558–70. [PubMed: 25176655]
39. Jeon JS, Zervantonakis IK, Chung S, Kamm RD, Charest JL. In vitro model of tumor cell extravasation. *PLoS One*. 2013; 8:e56910. [PubMed: 23437268]
40. Gorelik E, Wiltrot RH, Okumura K, Habu S, Herberman RB. Role of NK cells in the control of metastatic spread and growth of tumor cells in mice. *Int J Cancer*. 1982; 30:107–112. [PubMed: 7118294]
41. Labelle M, Hynes RO. The initial hours of metastasis: the importance of cooperative host-tumor cell interactions during hematogenous dissemination. *Cancer Discov*. 2012; 2:1091–9. [PubMed: 23166151]
42. Destaing O, et al. β 1A Integrin Is a Master Regulator of Invadosome Organization and Function. 2010; 21:4108–4119.
43. Stoletov K, Montel V, Lester RD, Gonias SL, Klemke R. High-resolution imaging of the dynamic tumor cell vascular interface in transparent zebrafish. *Proc Natl Acad Sci U S A*. 2007; 104:17406–11. [PubMed: 17954920]
44. Weis S, Cui J, Barnes L, Cheresh D. Endothelial barrier disruption by VEGF-mediated Src activity potentiates tumor cell extravasation and metastasis. *J Cell Biol*. 2004; 167:223–9. [PubMed: 15504909]
45. Kienast Y, et al. Real-time imaging reveals the single steps of brain metastasis formation. *Nat Med*. 2010; 16:116–22. [PubMed: 20023634]

46. Haidari M, et al. Integrin $\alpha 2\beta 1$ mediates tyrosine phosphorylation of vascular endothelial cadherin induced by invasive breast cancer cells. *J Biol Chem.* 2012; 287:32981–92. [PubMed: 22833667]
47. Maschler S, et al. Tumor cell invasiveness correlates with changes in integrin expression and localization. *Oncogene.* 2005; 24:2032–41. [PubMed: 15688013]
48. Yurchenco PD. Basement membranes: Cell scaffoldings and signaling platforms. *Cold Spring Harb Perspect Biol.* 2011; 3:1–27.
49. Mueller SC, et al. A Novel Protease-docking Function of Integrin at Invadopodia. *J Biol Chem.* 1999; 274:24947–24952. [PubMed: 10455171]
50. Sameni M, Dosescu J, Yamada KM, Sloane BF. Functional live-cell imaging demonstrates that beta(1)-integrin promotes type IV collagen degradation by breast and prostate cancer cells. 2009; 7:199–213.

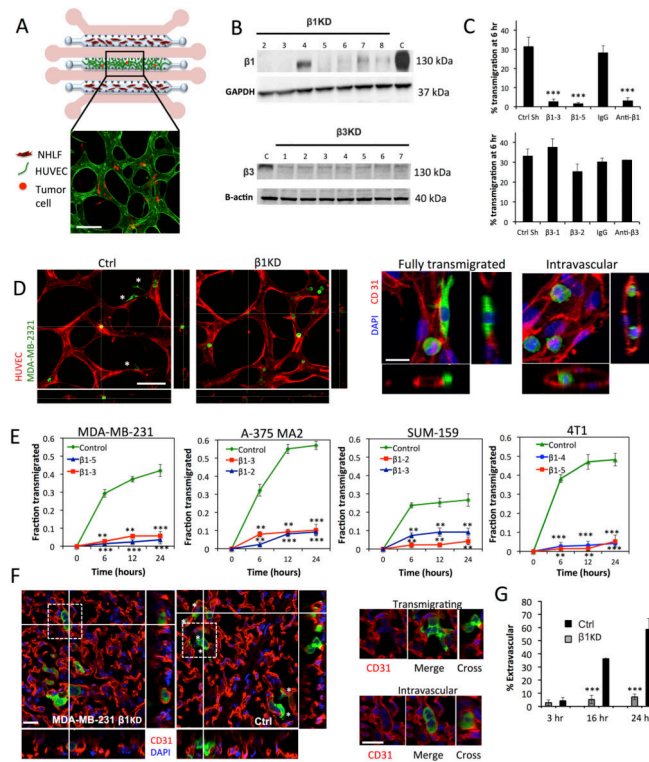


Fig 1. Knockdown of $\beta 1$ integrin inhibits tumor-cell transendothelial migration in *in vitro* microvascular networks and *in vivo* extravasation assays

(A) Schematic (not to scale) of the microfluidic device for the formation of microvascular networks. A central gel region with suspended human umbilical cord vein cells (HUVECs) is flanked by two normal human lung fibroblast (NHLF) channels. Each gel region is flanked by two media channels (pink). Representative fluorescence image of a single field of view of the device at 20X (HUVEC LifeAct; green, MDA-MB 231; red, scale bar = 100 μm). (B) Western blot of $\beta 1$ and $\beta 3$ integrin expression after suppression via shRNA (C=control shRNA targeting firefly luciferase). (C) Effect of $\beta 1$ and $\beta 3$ knockdowns and integrin function-blocking antibodies on the TEM efficiency of MDA-MB 231 in *in vitro* microvascular networks at 6 hours (** $p < 0.001$). (D) Representative field of views (20X) of live microvascular networks at 12 hr after seeding of control or $\beta 1$ KD MDA-MB-231 cells (HUVEC; red, MDA-MB 231; green). Asterisks indicate fully transmigrated cells (scale bar = 100 μm). Immunostaining for CD31 show distinctions between transmigrated and non-transmigrated cells (scale bar = 20 μm). (E) Differences in kinetics of TEM between $\beta 1$ KD and control shRNA cells were assessed for MDA-MB-231, A375 MA2, SUM-159 and 4T1 cells lines. Fraction transmigrated in human microvascular network devices is determined at the same field of view for time points of 0, 6, 12 and 24 hr ($n=3$, ** $p < 0.01$, *** $p < 0.001$, bars represent mean \pm SEM). (F) Immunostaining for CD31 (red) in mouse lungs 24 hours after injection of 0.5 million MDA-MB 231 control or $\beta 1$ KD cells (green). Asterisks indicate cells scored as transmigrated (scale bars = 20 μm). Cells in white dotted boxes are zoomed in to indicate examples of intravascular and extravascular cells. (G) Percentage of transmigrated control and $\beta 1$ KD MDA-MB 231 cells in mice lungs 3hr, 16 hr and 24 hr after tail vein injection ($n=8$ mice per condition at 3 hr and 24 hr, 4 mice per condition at 16

hr, 100 randomly selected tumor cells analyzed per mouse) (** $p < 0.001$, bars represent mean \pm SEM).

Author Manuscript

Author Manuscript

Author Manuscript

Author Manuscript

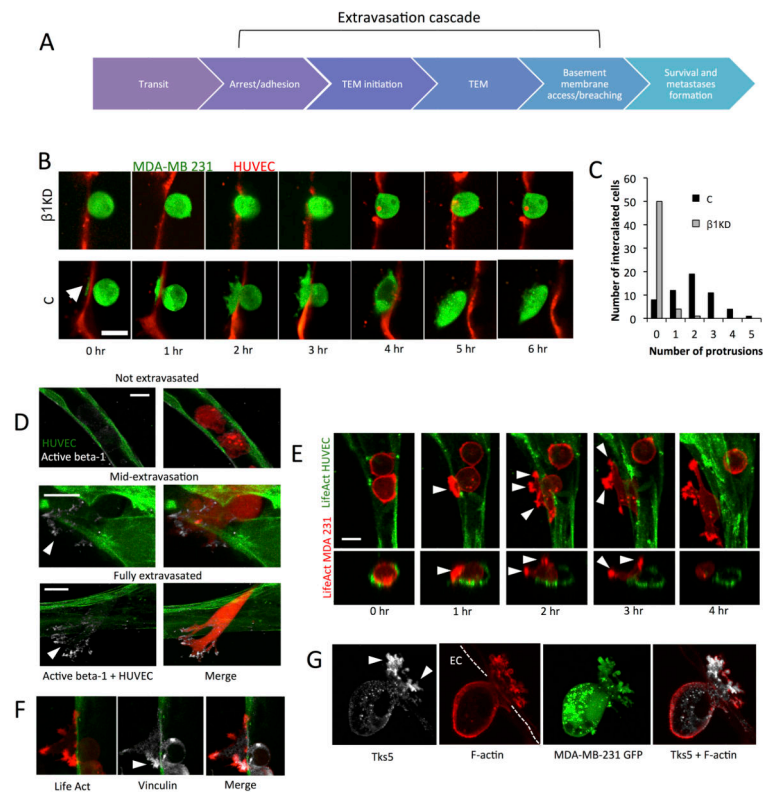


Fig 2. Activated $\beta 1$ and actomyosin rich protrusion formation precede and are required for complete transmigration

(A) Depiction of the multiple steps involved in the extravasation cascade. Circulating tumor cells arrest due to tumor-endothelium adhesion or size restriction. This is followed by onset of TEM, which may involve initiation of protrusions breaching an originally intact endothelium. After complete TEM, tumor cells may invade past the vascular basement membrane. (B) Time-lapse confocal microscopy of representative transmigrating control and $\beta 1$ -5 KD cells (single plane) over a period of 6 hours (HUVEC cell tracker; red, MDA-MB 231; green, scale bar=15 μ m). Arrow indicates the formation of initial protrusions into the subendothelial matrix in control cells. (C) Differences between control and $\beta 1$ -5 KD cells in the frequency of protrusion formation in single cells during TEM at 3 hours (55 intercalated cells over 3 devices per condition were chosen randomly and scored). Protrusion number (that was definable at 30X magnification) was quantified via 3D reconstructions of single transmigrating cells. (D) Immunostaining with an antibody against the activated conformation of $\beta 1$ integrin (clone 12G10, white) in microvascular networks (green) (scale bar = 10 μ m). Arrows indicate localization at protrusion tips. (E) Time-lapse imaging depicting spatial organization of tumor F-actin (red) during TEM in microvascular network devices. Arrows indicates areas in protrusions where F-actin appears as punctates (scale bar = 10 μ m). (F-G) Immunostaining of vinculin and Tks-5 in tumor cells during mid-transmigration past the endothelium. Arrows indicate localization of indicated proteins at the protrusion tips (scale bars = 10 μ m).

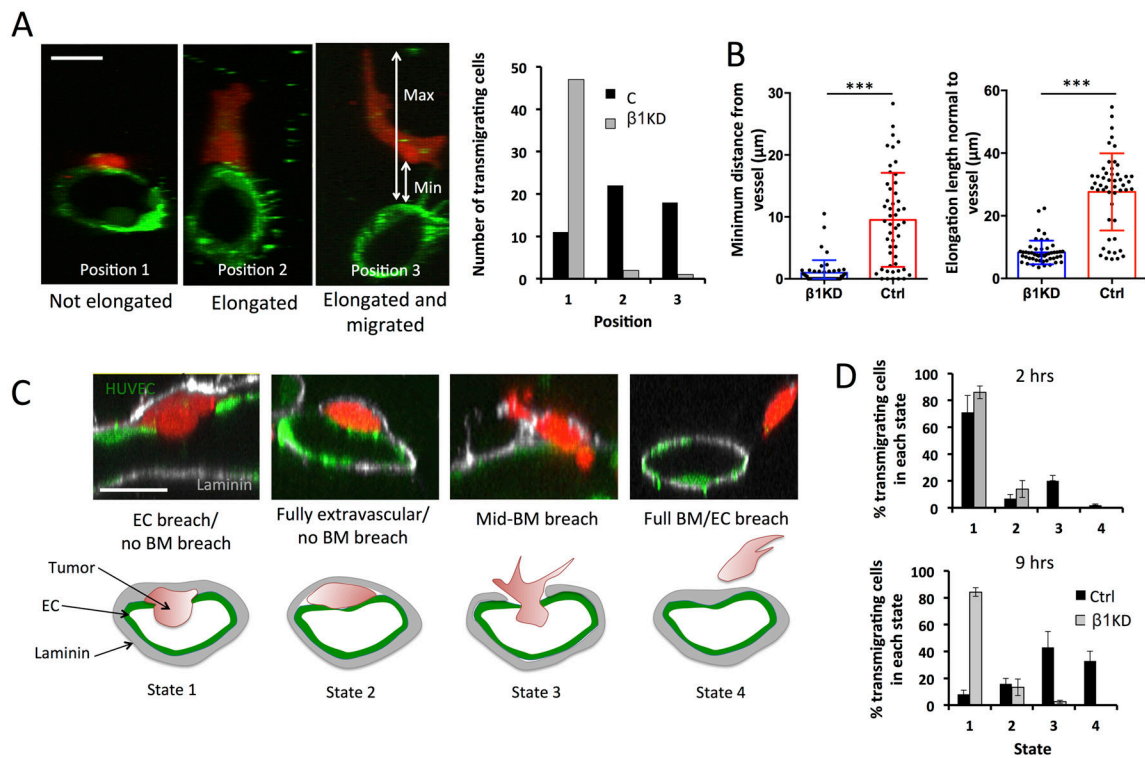


Fig 3. $\beta 1$ integrins mediate invasion past the basement membrane

(A) Representative cross sections of lumens in microvascular devices (scale bars = 10 μm) depicting the 3 distinct states in which a transmigrated tumor cell can be found relative to the endothelium after 6 hours (Position 1: directly adjacent to abluminal surface, Position 2: adjacent and elongated normal to vessel wall, Position 3: migrated away from the endothelium) (scale bars = 10 μm). Quantification of the number of fully transmigrated $\beta 1$ KD or control cells found in each “state” (50 cells analyzed per condition). (B) Quantification of the migration distance of extravasated tumor cells away from the endothelium. Distance is defined as the shortest length between the endothelium (at the point where transmigration occurred) and the nearest point on the transmigrated tumor cell body. Elongation length of the same transmigrated tumor cells is defined as the maximum length of the cell normal (perpendicular) to the vessel wall at the point of transmigration (n=50 transmigrated cells per condition, ***p<0.001, bars represent mean \pm standard deviation). (C) Representative immunofluorescence staining depicting the possible position of transmigrated tumor cells relative to the sub-endothelial laminin layer (LN: white, HUVEC LifeAct: green, MDA-MB 231: red, scale bars=10 μm). State 1: breached ECs but not laminin, State 2: fully transmigrated but no breaching of laminin, State 3: simultaneously breaching EC and laminin layer, State 4: fully breached EC and laminin layers. (D) Percentage of total fully transmigrated control or total $\beta 1$ -5 KD cells that are found in states 1 to 4 relative to the laminin layer (n=2 experiments, 4 devices per condition).

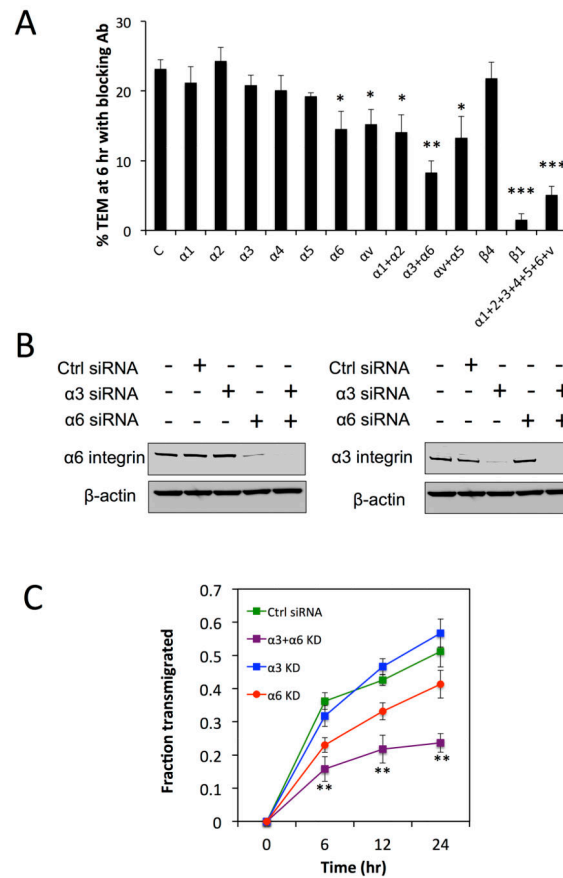


Fig 4. Transendothelial migration is mediated by $\alpha 3\beta 1$ and $\alpha 6\beta 1$ integrins via interactions with laminin
(A) Percentage transendothelial migration in microvascular network devices at 6 hours when tumor cells are treated with function-blocking antibodies for various α and β subunits (n=3 experiments, 3 devices per condition, *p<0.05, **p<0.01, ***p<0.001, bars represent mean +/- SEM). **(B)** Western blot analysis of alpha 3 and alpha 6-integrin individual knockdowns and co-knockdowns in MDA-MB-231 via siRNA. **(C)** Kinetics of TEM in microvascular networks following the same regions at 0, 6, 12 and 24 hr after tumor cell seeding.

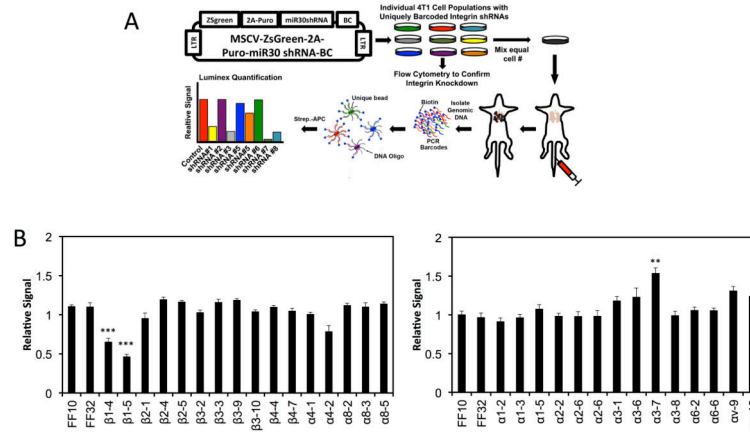


Fig 5. Knockdown of $\beta 1$ integrin in 4T1 cells inhibits metastatic colonization

(A) Schematic of our Luminex-based approach for multiplexing tail vein metastasis assays (see Methods). 4T1 cells were stably transduced with uniquely barcoded (*BC*) vectors expressing miR30-based shRNAs targeting one integrin subunit per cell population, and knock down was confirmed by flow cytometry (see Table 1). Uniquely barcoded 4T1 integrin knockdown cell populations were then mixed in equal numbers and injected into the tail veins of syngeneic Balb/C mice. After 17 days, Genomic DNA was isolated from the metastasis-containing lungs, and the relative amount of each barcode (i.e. the relative number cells expressing each shRNA) was quantified using streptavidin-conjugated APC (*Strep-APC*) and the Luminex FlexMap 3D system. (B) Luminex-based quantification of the relative metastatic burden of each 4T1 integrin knockdown cell population. Graphs show the relative signal + S.E.M. from each shRNA relative to the signal for that shRNA in the starting mixed population (n=10 mice / mix analyzed in duplicate).

Proposed molecular players in tumor transendothelial migration

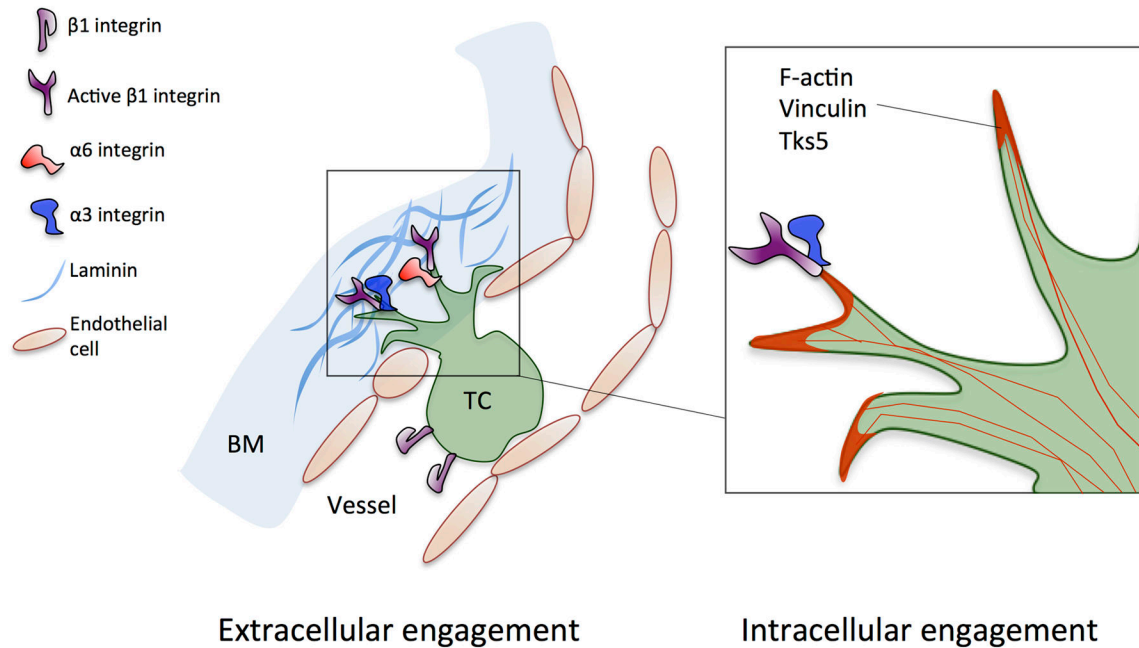


Fig 6. Proposed molecular players involved in tumor transendothelial migration

Extracellular engagement: activation of $\beta 1$ integrin facilitates protrusion maintenance past retracted endothelium, via engagement to subendothelial ECM. Specifically, integrins $\alpha 3\beta 1$ and $\alpha 6\beta 1$ are both required for adhesion to vascular basement membrane laminin.

Intracellular engagement: $\beta 1$ integrin-rich extracellular adhesions maintain protrusions, allowing focal adhesion proteins (e.g. vinculin) and F-actin to be recruited to the tips of protrusions, resulting in transmigration via acto-myosin contraction at the protruding edge.